# Correlation properties of MHD turbulence

A. Gurevich, K. Zybin, A. Luk'yanov

*P. N. Lebedev Physics Institute, Academy of Sciences of the USSR, Moscow*

R. Nebel

*Los Alamos National Laboratory, Los Alamos, New Mexico*

(Submitted 24 April 1991)
Zh. Eksp. Teor. Fiz. **100**, 1767–1780 (December 1991)

The correlation function of the MHD turbulence excited by a current in a thin, axisymmetric toroidal system is studied. The example of a reversed-field pinch is used to clarify the conditions under which anomalous transport arises. The dependence of the correlation function on the conditions at the boundary of the stochastic zone is studied. An accurate calculation of the correlation function is compared with an analytic expression for this function and good agreement is found.

## 1. INTRODUCTION

The problem of anomalous transport in toroidal magnetic confinement systems is of fundamental importance to success in the effort to achieve controlled fusion. It has been established that this anomalous transport is a consequence of the onset of turbulence in the plasma. Despite the turbulence which is excited, the plasma is in a quiescent state and, in a sense, a stable state. When the density and temperature of the plasma in steady state are given localized perturbations, for example, the perturbations are quickly smoothed out. Under certain conditions this stable stage becomes unstable. A sharp eruption of plasma or oscillations of the relaxation type occur, for example, so-called "saw-tooth" oscillations.[1,2]

Therefore the plasma turbulence which determines the anomalous transfer is characterized, in general, by the stable stage. The amplitudes of the stochastic oscillations of electric and magnetic fields in this situation are small compared to the basic microscopic fields:

$$e/E \ll 1, \quad b/B \ll 1. \tag{1}$$

There is another peculiarity—low frequency oscillations or, which is the same—not high velocity of the excitable waves compared with the heat velocity of electrons and ions:

$$v_f/v_t \ll 1, \quad v_t = v_{te}, \; v_{ti}. \tag{2}$$

The theory of plasma turbulence and the anomalous transfer processes is constructed through the use of an expansion in the small parameters in (1). The overall system of equations splits up into equations for the waves [these equations include terms both linear and nonlinear (usually quadratic) in the amplitudes $b$ and $e$] and equations for average macroscopic quantities. Generally speaking, the latter equations are written at the kinetic level. If the particle collisions are sufficiently effective, a system of hydrodynamic equations for the bulk plasma and separate equations for superthermal particles can be identified from the kinetics in the standard way.[3,4]

In this case the anomalous-transport processes are determined completely by the interaction of the particles with the waves. These processes are described by a "collision integral" $I_f$ which is nonlocal. Generally speaking, therefore, there is no way to reduce the anomalous-transport processes to a simple renormalization of the coefficients for ordinary collisional transport in a plasma. In addition, the collision integral representing the collisions with the waves, $I_f$, turns out to depend on the configuration of the average field $B(r)$. This dependence gives rise to strong nonlinear coupling in the system: The anomalous transport determines the configuration of the average macroscopic fields, which in turn have an inverse effect on the same transport processes, in this case at the level of the collision integral $I_f$. In addition, the configuration of the average fields strongly influences the excitation of the plasma waves themselves.[3,4]

We restrict the analysis here to MHD turbulence. This turbulence is excited effectively in a thin, axisymmetric toroidal system if the Kruskal-Shafranov condition is not satisfied.[5] This is the situation, in particular, in a reversed-field pinch (RFP). In a tokamak, the field $B_z$ (along the axis of the torus) set up by the external currents is an order of magnitude stronger than the field $B_\theta$ produced by the current in the plasma. In an RFP, $B_z$ and $B_\theta$ are on the same order of magnitude. The field $B_z$ falls off rapidly in magnitude along the radius $r$ of the torus, vanishing at a certain point $r_c$ in the plasma. Beyond this point the field $B_z$ changes sign; hence the name "reversed-field pinch" (Fig. 1). In a toroidal system there are resonant surfaces defined by the condition

$$k(r) = \frac{mB_\theta(r)}{rB(r)} + \frac{nB_z(r)}{RB(r)} = 0, \qquad B(r) = (B_z^2 + B_\theta^2)^{1/2}. \tag{3}$$

Here $m$ and $n$ are arbitrary integers, and $R$ is the major radius of the torus. The velocity of Alfvén waves vanishes on these resonant surfaces, because of the relation $V_a \sim k$. Consequently, when there are resonant surfaces in a toroidal system, slow modes satisfying the condition (2) may exist. These are approximately Alfvén modes, and they are localized for the most part near the corresponding resonant surfaces. A tokamak lacks the $m = 1$ resonant surfaces which play a major role in the excitation of an MHD turbulence. As a result, the Kruskal-Shafranov condition is satisfied, guaranteeing the overall MHD stability of the plasma. If an $m = 1, n = -1$ resonance appears in the central part of the

 0038-5646/91/120976-08$03.00  

discharge as a result of current peaking, disruptive oscillations are excited in the tokamak.[2] In an RFP, in contrast, the number of resonant surfaces is large. For the fundamental $m = 1$ mode these surfaces usually begin at $r_{1,n} \sim 0.1$–$0.3$. They become closely spaced near the reversal point $r_c$ (Fig. 1).

The presence and structure of the resonances and the configuration of the main field determine the excitation and basic properties of an MHD turbulence in an RFP. In the relaxed steady state, the turbulence has a steady-state spectrum of excited harmonics, and the interaction of the waves with the particles is described by only a single correlation function, $F(r)$, which completely determines the collision integral $I_f$. A remarkable property of the relaxed state in an RFP is the pronounced stability of the profile of the current and the magnetic field in the discharge.[6] The theory explains this stability on the basis that, although the profile is determined by the anomalous current transport, it is surprisingly insensitive to the particular type of MHD turbulence, i.e., to the function $F(r)$ (Refs. 7 and 8). In order to describe other transport processes, however, in particular, the loss of heat and plasma particles, we need to know the exact correlation function $F(r)$ and its properties for the fast-particle distribution. This information is also important for determining whether it is indeed possible to construct a differential description of the transport processes in a turbulent plasma. There are also the questions of determining the correlation function for spatially localized turbulence, which is precisely the case which prevails in RFPs and other toroidal systems.

The only way to answer these questions is to carry out a specific analysis of the correlation properties of MHD turbulence. These properties are the subject of the present paper.

## 2. CORRELATION INTEGRAL

The integral representing the scattering of particles by magnetic-field fluctuations is[4]

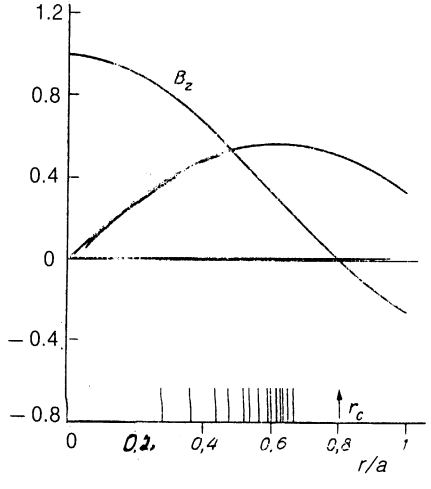


FIG. 1. Structure of the unperturbed magnetic fields $B_z$ and $B_\theta$ in a reversed-field pinch (RFP). The vertical lines show resonances; the arrow indicates $r_c$, which is the point at which the field $B_z$ reverses.

$$I_f = \frac{1}{r}\frac{\partial}{\partial r}(r\Gamma) + \tilde{I}_f,$$

$$\Gamma = \left\langle \int_0^\infty d\tau \int_{-\infty}^{+\infty} b_r b_r' G(\Omega|\Omega') \frac{\partial f}{\partial r'}(\Omega') d\Omega' \right\rangle. \tag{4}$$

Here $b_r$ represents the fluctuations of the magnetic field, $f(\Omega')$ is the distribution function, $\Omega'$ is the set of phase variables, $d\Omega'$ is an element of the phase volume, and $G(\Omega|\Omega')$ is the Green's function of a particle. This function describes the motion of the particle along a magnetic field line. For simplicity we have written out explicitly in expression (4) only a single term: that responsible for the spatial transport. Here $\tilde{I}_f$ represents the other terms.[7,8]

If the distribution function $f(\Omega')$ varies only slowly over a length scale $L_{\rm cor}$ ($L_{\rm cor}$ is the length scale of the decay of $\langle b_r b_r' \rangle$ along a field line), we find a diffusive expression for the flux $\Gamma$ through an expansion in the parameter $L_{\rm cor}|\mathbf{h}\nabla \ln f| \ll 1$, where $\mathbf{h} = \mathbf{B}_r/B$, from (4):

$$\Gamma = \int_0^\infty d\tau \int_{-\infty}^{+\infty} \langle b_r b_r' \rangle G(\Omega|\Omega') d\Omega' \frac{\partial f}{\partial r}. \tag{5}$$

Under these conditions, the correlation function is important in determining the anomalous transport. This correlation function is given by, according to (5),

$$F(r) = \int_0^\infty \langle b_r(r) b_r(r') \rangle dL, \tag{6}$$

$$\frac{dr'}{dL} = \frac{b_r(r', \theta', z')}{B}, \quad \frac{dz'}{dL} = \frac{B_z(r', \theta', z')}{B}, \quad \frac{d\theta'}{dL} = \frac{B_\theta(r', \theta', z')}{B}. \tag{7}$$

With $L = 0$ we have $r' = r$, $\theta' = \theta$, $z' = z$. Here $r$, $\theta$, $z$ are cylindrical coordinates; $L$ is the coordinate along a magnetic field line, with origin at the point $r, \theta, z$; and $B_\theta(r)$ and $B_z(r)$ are components of the main magnetic field $B = \sqrt{B_z^2 + B_\theta^2}$.

Equations (7) describe a magnetic field line in the case in which it is perturbed by a random field $b$. As in (4), the angle brackets mean an average over an ensemble of realizations of the random quantity $b_r$, in particular, over the initial values $\theta$ and $\Psi = z/R$; $\theta$, $\Psi \in [0, 2\pi]$.

The approximation of cylindrical symmetry is valid for a thin toroid if its minor radius $a$ is much smaller than the major radius $R$ of the torus. In this case the field $b_r$ in the toroid can be represented by a Fourier series in $\theta$ and $z$:

$$b_r = \sum_{mn} b_r^{mn}(r) \exp(i(m\theta + \Psi n)). \tag{8}$$

If the field fluctuations $b_r$ are ignored in Eqs. (7), then by substituting (8) into (6) and taking an average over $\theta$ and $\Psi$ we find

$$F(r) = 2\pi \sum_{mn} |b_r^{mn}(r)|^2 \delta\left(\frac{mB_\theta}{rB} + \frac{nB_z}{RB}\right). \tag{9}$$

In (9) we have used $|b_r^{mn}| = |b_r^{-m-n}|$; the terms with $-m$ and $-n$ are not summed.

It follows from (9) that if we ignore perturbations of the field lines of the random magnetic field then the entire correlation function $F(r)$ is concentrated at the resonant surfaces. In other words, this function exists only as a set of isolated peaks. This result means that there is no anomalous transport in the interior of the plasma, where the MHD oscillations are excited. This anomalous transport appears only if the resonances overlap, since only in this case do the field lines undergo a random walk.

To find the conditions under which the resonances overlap, we seek a solution of Eqs. (7) near the resonant surfaces. Substituting (8) into (7), and retaining only the resonant mode, we find

$$\frac{dr'}{dL} = \frac{b_r^{mn}(r')\exp\left(i\left(m\theta' + \frac{n}{R}z'\right)\right)}{B} + \text{c.c.},$$

$$\frac{dz'}{dL} = \frac{B_z}{B}, \quad \frac{d\theta'}{dL} = \frac{B_\theta}{r'B}. \tag{10}$$

We write the coordinate $r'$ as $r' = r + \rho(L)$, and we consider the case in which the broadening of the resonances satisfies $\delta r \sim \rho(L) \sim \Delta r_{mn}$, where $\Delta r_{mn} \ll a$ is the distance between resonances (the length scale of the variations in the main field). We then find

$$\frac{d\rho}{dL} = \frac{b_r^{mn}}{B}\exp\left(i\left(m\theta' + \frac{n}{R}z'\right)\right) + \text{c.c.},$$

$$\frac{d\theta'}{dL} = \frac{h_\theta(r)}{r} + \left(\frac{h_\theta(r)}{r}\right)'\rho, \quad \frac{dz'}{dL} = h_z(r) + h_z'\rho, \tag{11}$$

where $h'_{\theta,z}$ is the derivative of the functions $h_{\theta,z} = B_{\theta,z}/B$ with respect to $r$.

At this point it is convenient to introduce the function $g(L)$:

$$g = \int_0^L \rho(L')dL'.$$

Working from (11), we then find

$$\theta' = \theta + \frac{h_\theta}{r}L + \left(\frac{h_\theta}{r}\right)'g, \quad z' = z + h_z L + h_z' g. \tag{12}$$

Substituting (12) into (11), we find an equation for the function $g$:

$$\frac{d^2g}{dr^2} = \frac{b_r^{mn}}{B}\exp\left(i\left(m\theta + \frac{n}{R}z + kL + k'g\right)\right), \tag{13}$$

$$g(0) = 0, \quad g'(0) = 0.$$

The quantity $k$ in (13) is defined by (3), and $k'$ is the derivative of the function $k$ with respect to $r$, as in (11). Near the resonant surface we have $k \approx 0$. Setting $k'g \ll 1$, we find

$$g = \left|\frac{b_r^{mn}}{B}\right| L^2 \sin\left(m\theta + \frac{n}{R}z + \mu_{mn}\right). \tag{14}$$

Here $\mu_{mn}$ are the phases of the random field $b_r^{mn}$, which is given by $b_r^{mn} = |b_r^{mn}|\exp(i\mu_{mn})$. Expanding (6) in a Fourier series, and substituting (12) and (14), we find

$$F = \left\langle \sum_{mnm'n'} \int_0^\infty b_r^{mn}(r)\, b_r^{m'n'}(r')\exp\left(i\left(m\theta + m'\theta + \frac{n'}{R}z + \frac{n}{R}z + k(r)L + k'g\right)\right)dL \right\rangle. \tag{15}$$

Let us examine the behavior of the correlation function $F(r)$ as a function of the phase $\mu_{mn}$. We first set $\mu_{mn} + m\theta + \Psi n = \pi/2$; i.e., we fix the phase. Expression (15) then becomes

$$F = 2\sum_{mn}\int_0^\infty |b_r^{mn}|^2 \cos\left(k'L\delta r + k'\left|\frac{b_r^{mn}}{B}\right|L^2\right)dL, \tag{16}$$

where $g(L)$ is taken from (14) with $\mu_{mn} + m\theta + \Psi n = \pi/2$, the quantity $k$ has been expanded in $\delta r = r - r_{mn}$ (the excursion from the resonance point), and the summation rule is similar to that in (9). Evaluating the integral in (16) in the WKB approximation, we finally find

$$F(r) = [\pi B(r)]^{1/2}\sum_{mn}|b_r^{mn}|^2\frac{\cos y^2}{(k'|b_r^{mn}|)^{1/2}},$$

$$y^2 = (r - r_{mn})^2\left|\frac{Bk'}{8b_r^{mn}}\right|. \tag{17}$$

Since (17) is valid only in a small neighborhood of each resonance, it is natural to set $\cos(y^2) = 0$ at $y^2 > \pi/2$ (Ref. 8).

In another approximation, we assume that the phases $\mu_{mn}$ are random; we integrate over the random phases $\mu_{mn}$ in (15) and then take averages over $z$ and $\Psi$. As a result we find

$$F(r) = 2\sum_{mn}|b_r^{mn}|^2\int_0^\infty J_0(\varkappa L^2)\cos(k'\delta r L)\,dL,$$

$$\varkappa = \left|\frac{k'b_r^{mn}}{B}\right|, \quad \delta r = r - r_{mn}, \tag{18}$$

where $k$ is given by (3), $J_0$ is the Bessel function of order zero as in (17), $k' = dk/dr|_{r=r_{mn}}$, the resonance points $r_{mn}$ are found from (3), and the summation rule is like that in (9).

We have written two expressions for the correlation function. Expression (17) was derived at a fixed phase of the fields $b_r$, while expression (18) was derived by taking an average over the random phases $\mu_{mn}$. We will see below (Fig. 9) that these approximate expressions do not differ greatly from each other or from the accurate value of the correlation function. The expression given in Ref. 7 for the correlation function is incorrect (see Ref. 8). First, however, we would like to discuss some important general correlation properties of fluctuations which are excited in a bounded discharge volume.

## 3. CORRELATION PROPERTIES OF SPATIALLY LOCALIZED TURBULENCE

The resonant surfaces in an RFP lie inside the reversal point, at $r < r_c$. At the center of the discharge there are no

resonances, because of the cylindrical symmetry. All the magnetic field lines thus undergo random walk in a bounded volume (Fig. 1).

The general expression for the collision integral representing the collisions of particles with fluctuations, $I_f$ [see (4)], is generally nonlocal in form. As we mentioned earlier, this expression becomes a diffusion-like expression under the condition $L_{cor} \ll L$, where $L = |f/h\nabla f|$. From expression (5) for the diffusive flux we then find an equation for the mean square displacement of a particle:

$$\frac{d}{dL}\langle (r-r_0)^2\rangle = \frac{F}{B^2}. \tag{19}$$

Here $r_0$ is the point from which the displacement begins. Integrating (19), we find

$$\langle (r-r_0)^2\rangle = \int_0^L \frac{F(L')}{B^2}\, dL'. \tag{20}$$

In an unbounded space, as $L \to \infty$, we then find the usual diffusion law $\langle (r-r_0)^2\rangle = FL/B^2$, but in a bounded volume we find $\langle (r-r_0)^2\rangle \leqslant a^2$, where $a$ is the scale length of the localization of the fluctuation region. From (20) we thus find

$$F(L) \to 0 \tag{21}$$

as $L \to \infty$. In the case of turbulence excited in a bounded volume, calculation of the correlation function from (6) thus yields $F(r) = 0$. This result definitely does not mean that the diffusion coefficient tends toward zero, of course. To illustrate the latter assertion, we consider the diffusion of particles in a bounded volume $r \in [-a, a]$. The equation describing the diffusion is

$$\frac{\partial N}{\partial L} = D\frac{\partial^2 N}{\partial r^2}. \tag{22}$$

Under the assumption that the particles do not leave the given volume, we find that the flux $D\partial N/\partial r$ vanishes at $r = \pm a$. Assuming that the initial distribution $N_0(r)$ is symmetric, we find the following solution of the diffusion equation (22):

$$N = \sum_{n=0}^{\infty} C_n \cos\left(\frac{\pi r}{a} n\right) \exp\left[-\left(\frac{\pi n}{a}\right)^2 DL\right]. \tag{23}$$

In particular, if $N_0(r) = \delta(r)$, all the constants $C_n$, $n = 1,\ldots$, describing the initial distribution are equal to unity, while $C_0 = 1/2$. The square displacement $\langle r^2\rangle$ is naturally found from

$$\langle r^2\rangle = \frac{\int_{-a}^{+a} r^2 N\, dr}{\int_{-a}^{+a} N\, dr}. \tag{24}$$

Using (24) and (23), we find

$$\langle r^2\rangle = \frac{a^2}{3} + 4\sum_{n=1}^{\infty} (-1)^n \left(\frac{a}{\pi n}\right)^2 \exp\left[-\left(\frac{\pi n}{a}\right)^2 DL\right]. \tag{25}$$

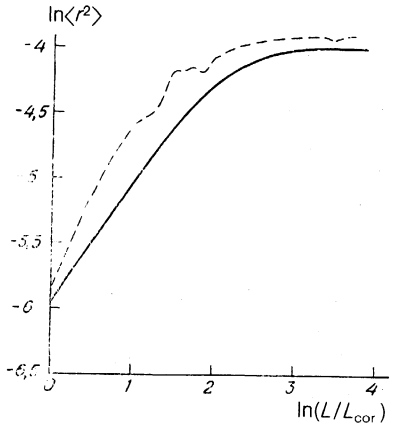


FIG. 2. Plot of $\ln\langle r^2\rangle$ versus $\ln(L/L_{cor})$. Solid line—Expression (25); dashed line—result of the numerical simulation for $N = 21$ resonances.

Figure 2 shows $\langle r^2\rangle$ versus $L$. As $L \to 0$ we find ordinary diffusion from (25). As $L \to \infty$, in contrast, we find from (23) and (24)

$$\frac{d}{dL}\langle r^2\rangle = 4D\frac{C_1}{C_0}\exp\left[-\left(\frac{\pi}{a}\right)^2 DL\right].$$

The diffusion coefficient can thus be determined most conveniently from the initial, linear part of the plot of $\langle r^2\rangle$ versus $L$, before it starts curving because of the boundary effect. It follows that in determining the correlation function $F(r)$ for spatially localized turbulence, we should integrate over $L$ in (6) not to infinity but to a certain $L_0$ which is greater than or equal to $L_{cor}$ but less than the length $L_w$, at which the boundary effect becomes important:

$$L_{cor} \leqslant L_0 \ll L_w. \tag{26}$$

Obviously, a differential description of the transport process for localized turbulence is legitimate only if this condition holds.

The expression for the correlation function may contain, in addition to the rapid decay at short distances $L \sim L_{cor}$, some slowly varying correlations. The integral representing the scattering of particles by fluctuations, in particular, the flux $\Gamma$, can thus be broken up into two parts in a natural way: $\Gamma = \Gamma_1 + \Gamma_2$, where

$$\Gamma_1 = \int_0^{\tau_{cor}} d\tau \int_{-\infty}^{+\infty} \langle b_r b_r'\rangle\, G(\Omega|\Omega')\, d\Omega' \frac{\partial f}{\partial r}, \tag{27}$$

$$\Gamma_2 = \int_{\tau_{cor}}^{\infty} d\tau \int_{-\infty}^{+\infty} \langle b_r b_r'\rangle\, G(\Omega|\Omega') \frac{\partial f}{\partial r'}\, d\Omega', \tag{28}$$

where $\Gamma_1$ is the ordinary diffusion flux, and the flux $\Gamma_2$ is determined by long-range correlations, which are nonlocal.

Let us examine the physical meaning of the flux $\Gamma_2$. The correlation function vanishes in (6) and (21) because once a trajectory (a magnetic field line) reaches the boundary it goes back into the turbulent plasma volume; it does this repeatedly as $L \to \infty$. For a trajectory undergoing a random

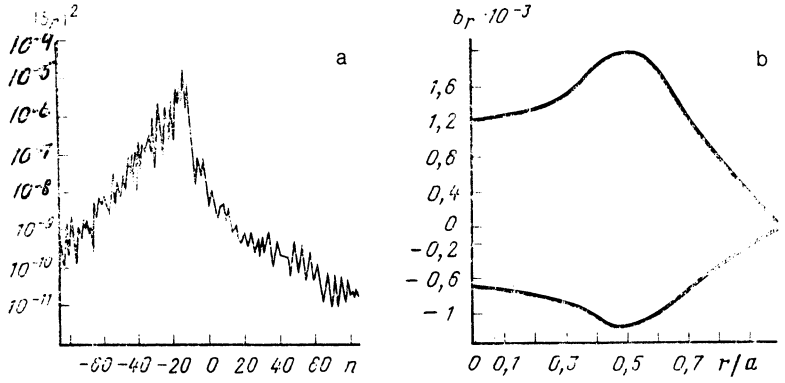


FIG. 3. a—Spectrum of MHD oscillations in an RFP and $|b_r^{mn}|^2$ versus the mode index $n$, with $m = 1$. b—The mode $b_r^{mn}$ as a function of $r$ for $m = 1$ and $n = -15$, as an example. Dashed line—Imaginary part; solid line—real part.

walk, an integration over $d^3r'$ in (28) is thus identical to an average of the flux $\Gamma_2$ over the entire volume. Far from the boundaries of the stochastic zone, expression (28) is therefore a constant, and its physical meaning is the diffusion flux through the plasma volume. Expression (28) changes only near the boundary, over a distance on the order of $L_{cor}$. This change depends strongly on whether the trajectory goes back into the volume or leaves it (there is a certain probability for the latter outcome).

The exact expression (4) for the integral representing the scattering of particles by fluctuations thus incorporates both the diffusive transport described by expression (27) and the boundary conditions which are specified by (28) in terms of the behavior of the trajectory near the boundary of the stochastic zone. We now illustrate these assertions using as an example the numerical analysis of MHD turbulence in an RFP.

#### 4. MHD TURBULENCE IN AN RFP

A $3D$ numerical simulation was carried out to study MHD turbulence in a reversed-field pinch (RFP). The MHD solutions were solved by the method described in Ref. 10, which involves a Fourier-series expansion in the coordinates $\theta$ and $z$ with the help of fast Fourier transforms. In general, the total number of Fourier harmonics was $N > 100$. This numerical calculation was carried out by one of the present authors on a Cray computer. The solution was carried out up to the time at which a steady-state mode spectrum was established. The computation time $t$ was greater than $\tau_r$, i.e., the time scale of the resistive diffusion in the system. Figure 3 shows a representative steady-state spectrum.

The behavior of the field lines in various zones of the discharge was studied through a direct numerical solution of Eqs. (7) for the field lines of the magnetic field $B = B_0(r) + \Sigma_{mn} b_r^{mn} \exp(i(m\theta + \Psi z)) + \text{c.c.}$, where the modes $b_r^{mn}$ were taken from the complete MHD calculation described above. As the main field $B_0(r)$ we used Taylor's solution, expressed in terms of Bessel functions: $B_z = B_0 J_0(\beta r/r_c)$, $B_\theta = B_0 J_1(\beta r/r_c)$, where $\beta$ is the first root of $J_0(x)$ (Ref. 11). Some examples are shown in Fig. 4. Outside the zone of the resonances (Fig. 1) the field lines exhibit genuinely dynamic behavior. In the zone of the resonances, in contrast, two field lines which initially run close together move apart exponentially, indicating dynamic chaos in this zone. Figure 5 shows a Poincaré section in the $r, z$ plane for the system (7). We see that for $0.2 < r < 0.8$ the magnetic surfaces are completely disrupted, so the trajectory of motion of a particle along a field line is stochastic. The stochastic properties of a model magnetic field in an RFP (with a very simple model form of the modes $b_r^{mn}$) were studied by a mapping method in Ref. 9.

We turn now to a direct calculation of the correlation function $F(r)$. Figure 6 shows the integrand $\langle b_r(r) b_r(r') \rangle$ as a function of $L$. The averaging indicated by the angle brackets was carried out for a given $r$ over the initial points $\theta_0$ and $z_0$ and also over the phases $\mu_{mn}$. As a result of the averaging, the function $\langle b_r(r) b_r(r') \rangle$ depends only on $L$ and the initial coordinate $r$. It can be seen from Fig. 6 that there are three regions on the plot of $\langle b_r(r) b_r(r') \rangle$ versus $L$.

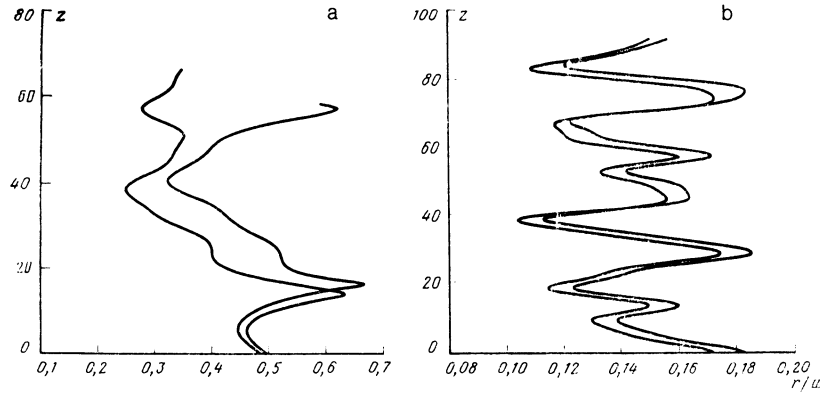


FIG. 4. Magnetic field lines in the $r z$ plane in an RFP. a—In the stochastic zone; b—outside the stochastic zone.

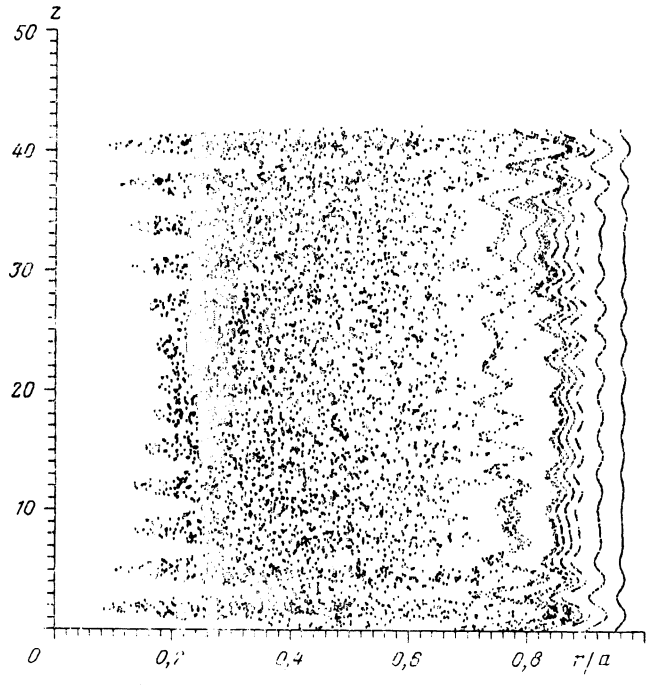


FIG. 5. Poincaré section in the $r z$ plane in an RFP.

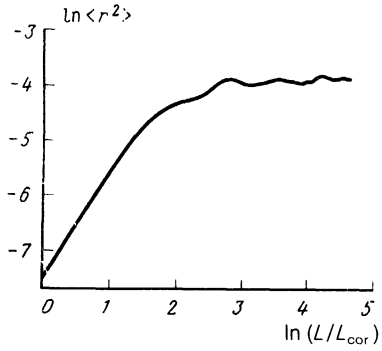


FIG. 7. Plot of $\ln\langle r^2\rangle$ versus $\ln L/L_{\text{cor}}$ in an RFP.

One region is a rapid decay of $\langle b_r(r)b_r(r')\rangle$ to zero over a length scale on the order of $L \approx L_{\text{cor}} \approx 5$–6. Another is a region of negative values of $\langle b_r(r)b_r(r')\rangle$, which varies rather slowly with $L$. This region extends to $L_W \approx 30$–50, telling us that a significant fraction of the trajectories reflected from the boundaries of the stochastic zone return. The point $L_W$, which corresponds to the vanishing of the correlation function $F(r) = \int_0^{L_W}\langle b_r(r)b_r(r')\rangle dL$, is shown by the arrow in Fig. 6. For $L > L_W$ there are some small oscillations in $\langle b_r(r)b_r(r')\rangle$, which reflect the presence of a regular structure near the boundary of the zone (Fig. 5).

We see that the numerical results are in total agreement with the analysis of the behavior of the correlation function carried out in the preceding section of this paper. In particular, the behavior of the quantity $\langle r^2\rangle = \int_0^L (F/B^2)\, dL$ shown in Fig. 7 agrees with (23) and (25). Another important point is that the integrand $\langle b_r(r)b_r(r')\rangle$ in the region $L > L_{\text{cor}}$ depends strongly on the nature of the boundary conditions. That this is true can be seen from Fig. 8, which shows the results of a calculation of $F(r) = \int_0^L \langle b_r(r)b_r(r')\rangle dL$ in a case with absorbing boundaries, i.e., $b_r(r)b_r(r') = 0$, when the trajectory reaches the boundary $r^+$ or $r^-$. We see that the main positive part of the correlation expression remains essentially constant, while the negative part gradually vanishes as the difference $r^+ - r^-$ decreases.

In determining the correlation function $F(r)$ we should thus carry out the integration in (6) only up to the value of $L$ set by the condition $\langle b_r(r)b_r(r')\rangle = 0$. This cutoff of the function $\langle b_r(r)b_r(r')\rangle$ was made in the direct calculation of the correlation function $F(r)$. We see that the calculated correlation function $F(r)$ is in reasonable agreement with the approximate analytic expressions (18) and (19) (Fig. 9). The observed discrepancy stems from the extent to which resonances overlap, which depends on the amplitudes of the harmonics, and also from the comparatively small number of resonant modes which actually determine the onset of the stochastic behavior of the field lines in this example.

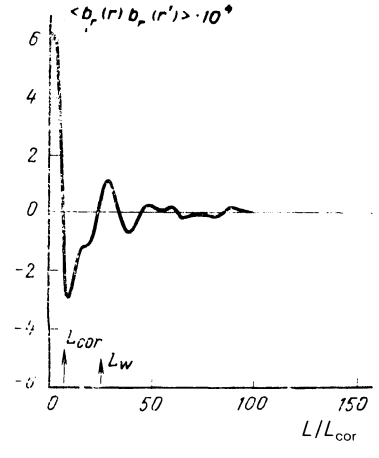


FIG. 6. The integrand $\langle b_r(r)b_r(r')\rangle$ versus $L/L_{\text{cor}}$.

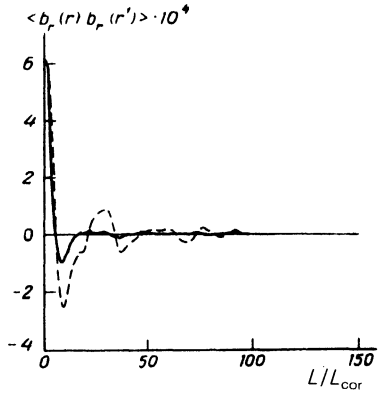


FIG. 8. The integrand $\langle b_r(r)b_r(r')\rangle$ versus $L/L_{\text{cor}}$ in the presence of absorbing boundaries $r^+$ and $r^-$. Dashed line—$r^+ = 0.7$, $r^- = 0.2$; solid line—$r^+ = 0.6$, $r^- = 0.3$.

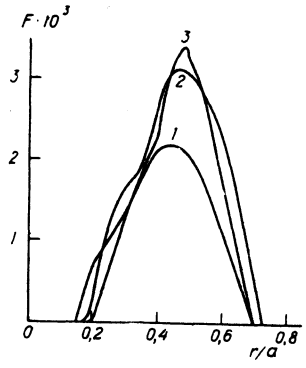


FIG. 9. The correlation function $F(r)$. 1—Numerical simulation; 2—calculated from expression (17); 3—calculated from (18).

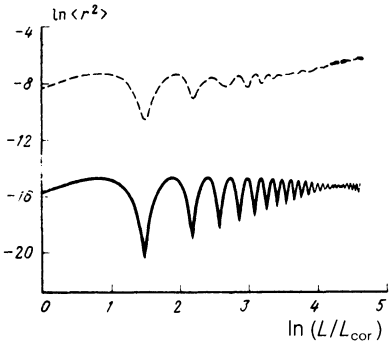


FIG. 11. Plot of $\ln\langle r^2\rangle$ versus $\ln\sim(L/L_{\rm cor})$. Dashed line—In the region of regular trajectories; solid line—at small values of the fluctuation amplitude.

We will therefore discuss the dependence of the correlation function $F(r)$ on the fluctuation amplitude and the number of resonances, $N$. Figure 10 shows the correlation function $F(r)$ calculated from (17) and (18) along with that found through the numerical simulation, versus the fluctuation amplitude $b$. We see that the discrepancy between the numerical simulation and expressions (17) and (18) disappears as the amplitude $b$ decreases, while the resonances remain overlapping. At sufficiently small amplitudes, for which neighboring resonances do not overlap, the $L$ dependence of $\langle r^2\rangle$ (Fig. 11) differs substantially from the diffusion-like behavior shown in Fig. 7. The behavior in Fig. 11 is similar to the dynamic $L$ dependence of $\langle r^2\rangle$ for the region of regular trajectories, which is shown in the same figure. As the number $N$ of resonances increases, the characteristic size of the region which comes before the first zero of the integrand becomes progressively smaller in comparison with the corresponding size of its negative part, $F(r)$ (Fig. 12).

We now let $N\to\infty$. With a stochastic region of finite volume, this limit means that the distance between resonances vanishes: $\Delta r_{mn}\to 0$. In this case we have $L_{\rm cor}\to 0$; i.e., the positive part of $\langle b_r(r)b_r(r')\rangle$ is expressed by a $\delta$-function. To determine the complete function, we go back to solution (27), in which the boundary conditions are taken into account. The motion of a particle in the field of "random velocities" is described by

$$r(L)=\int_0^L \frac{b_r(L')}{B}\,dL'. \tag{29}$$

Squaring (29) and taking an average, we find

$$\langle r^2(L)\rangle=\int_0^L dL_1\int_0^{L_1} dL_2\,\frac{\langle b_r(L_1)b_r(L_2)\rangle}{B^2}. \tag{30}$$

We see from (30) that the integrand $\langle b_r(0)b_r(L)\rangle$ is determined by

$$\frac{d^2\langle r^2\rangle}{dL^2}=\frac{\langle b_r(0)b_r(L)\rangle}{B^2},\quad L=L_1-L_2. \tag{31}$$

Using solution (25) and relation (31), we find

$$\frac{\langle b_r(0)b_r(L)\rangle}{B^2}=4D^2\sum_{n=1}^{\infty}(-1)^n\left(\frac{\pi n}{a}\right)^2\exp\left[-D\left(\frac{\pi n}{a}\right)^2 L\right]. \tag{32}$$

Figure 12 compares the analytic expression (32) for the function $\langle b_r(0)b_r(L)\rangle$ with the results of the direct numerical calculation of this function for a fairly large number of resonances. We see that there is a quantitative, not merely qualitative, agreement.

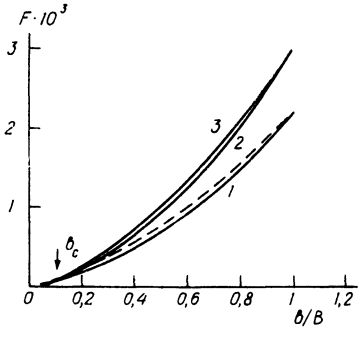


FIG. 10. The correlation function $F(r)$ at the point $r=0.43$ versus the oscillation amplitude $b$. 1—Numerical simulation; 2—calculation from expression (17); 3—calculation from expression (18); arrow—the amplitude $b_c$; dashed line—the function $W(b)=b^{a/2}2.2\cdot 10^{-2}$.

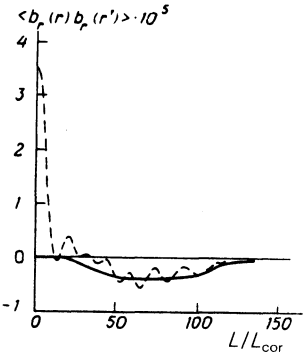


FIG. 12. The integrand $\langle b_r(r)b_r(r')\rangle$ versus $L/L_{\rm cor}$. Dashed line—Case of many resonances ($N=21$); solid line—calculated from (32).

From this analysis we can draw the following conclusions.

1. A differential description of the anomalous transport in the turbulent region which arises when the resonances overlap is legitimate only under the conditions $N \gg 1$ and $\delta r_{\max}/a \ll 1$, where $N$ is the number of resonances, $\delta r_{\max}$ is the maximum distance between resonances, and $a$ is the length scale of the variations in the distribution function $f$.

2. In defining the correlation function one should use not (6) but the formula

$$F(r) = \int_0^{L_0} \langle b_r b_r' \rangle \, dL,$$

where $L_0$ is the point at which the integrand $\langle b_r b_r' \rangle$ vanishes [see (26)]. The regular negative part of $\langle b_r b_r' \rangle$ which arises at $L > L_0$ is an effect of the boundaries of the turbulent region (Fig. 12). In a differential description of anomalous transport, this part is automatically incorporated in the boundary conditions (Fig. 8).

3. Analytic expressions (17) and (18) for the correlation function become progressively more accurate as the number of resonances $N$ increases and as the oscillation amplitude $b$ approaches the critical value $b_c/B \approx k' \delta r_{\max}^2/8$, at which only the nearest resonances overlap (Fig. 10). For $b < b_c$, the resonances do not overlap, and the anomalous transport vanishes (Fig. 11).

4. An analytic calculation of the correlation function from $F(r) = (b/b_c)F_b(r)$, where the function $F_b(r)$ is given by (17) and (18) with $b = b_c$, leads to a result which is essentially the same as the result of the numerical calculation (Fig. 10).

We wish to thank M. Ptitsyn and M. Stolyarov for assistance in the numerical calculations and for useful discussions.

[1] P. C. Liewer, Preprint, Department of Applied Physics, California Institute of Technology: A Review, 1984.
[2] S. V. Mirnov, *Physical Processes in Plasmas*, Energoatomizdat, Moscow, 1983.
[3] A. V. Gurevich, K. P. Zybin, and Ya. N. Istomin, Zh. Eksp. Teor. Fiz. **84**, 86 (1983) [Sov. Phys. JETP **57**, 51 (1983)].
[4] A. V. Gurevich, K. P. Zybin, and Ya. N. Istomin, Nucl. Fusion **27**, 453 (1987).
[5] V. D. Shafranov and É. I. Yurchenko, Zh. Eksp. Teor. Fiz. **53**, 1157 (1967) [Sov. Phys. JETP **26**, 682 (1968)].
[6] H. A. B. Bodin and A. A. Newton, Nucl. Fusion **20**, 1255 (1980).
[7] A. V. Gurevich, K. P. Zybin, and A. V. Luk'yanov, Zh. Eksp. Teor. Fiz. **97**, 468 (1990) [Sov. Phys. JETP **70**, 259 (1990)].
[8] A. Gurevich, A. Lukyanov, and K. Zybin, in *Proceedings of the Course and Workshop on Physics of Alternative Magnetic Confinement Schemes*, held at Villa Monastero, 15–24 October, Varenna, Italy, 1990.
[9] N. Reggiani and M. Malavasi, in *Proceedings of the Course and Workshop on Physics of Alternative Magnetic Confinement Schemes*, held at Villa Monastero, 15–24 October, Varenna, Italy, 1990.
[10] D. D. Schnack, D. C. Barnes, Z. Mikic, D. S. Harned, E. J. Caramana, and R. A. Nebel, Comp. Phys. Commun. **43**, 17 (1986).
[11] J. B. Taylor, Rev. Mod. Phys. **58**, 741 (1986).

Translated by D. Parsons